JBC ARTICLE

Diacylglycerol kinases regulate TRPV1 channel activity

Received for publication, December 30, 2019, and in revised form, April 24, 2020 Published, Papers in Press, April 28, 2020, DOI 10.1074/jbc.RA119.012505

Luyu Liu, Yevgen Yudin, and Tibor Rohacs*

From the Department of Pharmacology, Physiology, and Neuroscience, Rutgers New Jersey Medical School, Newark, New Jersey, USA

Edited by Roger J. Colbran

The transient receptor potential vanilloid 1 (TRPV1) channel is activated by heat and by capsaicin, the pungent compound in chili peppers. Calcium influx through TRPV1 has been shown to activate a calcium-sensitive phospholipase C (PLC) enzyme and to lead to a robust decrease in phosphatidylinositol 4,5-bisphosphate [$PI(4,5)P_2$] levels, which is a major contributor to channel desensitization. Diacylglycerol (DAG), the product of the PLC-catalyzed $PI(4,5)P_2$ hydrolysis, activates protein kinase C (PKC). PKC is known to potentiate TRPV1 activity during activation of G protein–coupled receptors, but it is not known whether DAG modulates TRPV1 during desensitization. We found here that inhibition of diacylglycerol kinase (DAGK) enzymes reduces desensitization of native TRPV1 in dorsal root ganglion neurons as well as of recombinant TRPV1 expressed in HEK293 cells. The effect of DAGK inhibition was eliminated by mutating two PKC-targeted phosphorylation sites, Ser-502 and Ser-800, indicating involvement of PKC. TRPV1 activation induced only a small and transient increase in DAG levels, unlike the robust and more sustained increase induced by muscarinic receptor activation. DAGK inhibition substantially increased the DAG signal evoked by TRPV1 activation but not that evoked by M1 muscarinic receptor activation. Our results show that Ca^{2+} influx through TRPV1 activates PLC and DAGK enzymes and that the latter limits formation of DAG and negatively regulates TRPV1 channel activity. Our findings uncover a role of DAGK in ion channel regulation.

The TRPV1 ion channel is a major noxious heat sensor; it is expressed in primary sensory neurons of the dorsal root ganglia (DRG) and trigeminal ganglia. TRPV1 is an outwardly rectifying nonselective cation channel with high permeability to Ca^{2+}; its activation depolarizes the neuron and induces a robust Ca^{2+} signal (1). In accordance with its role as a noxious heat sensor, activation of TRPV1 by capsaicin, the pungent compound in chili peppers, evokes a burning pain sensation.

Proinflammatory mediators such as bradykinin, prostaglandins, and extracellular ATP sensitize TRPV1 to activation by heat, capsaicin, and extracellular protons, which manifest as a left shift of the dose–response curves of these activators (2, 3). Most of these proinflammatory mediators exert their effects through activation of G protein–coupled receptors that act via $G\alpha_q$ and stimulate PLCβ enzymes. Sensitization of TRPV1 activity has been shown to be mediated mainly by phosphorylation of the channel by PKC at residues Ser-502 and Ser-800 (4). The *in vivo* relevance of phosphorylation of the Ser-800 residue (Ser-801 in mice) has also been demonstrated recently (5).

Upon sustained maximal stimulation by capsaicin, TRPV1 activity decreases despite the presence of the agonist, a phenomenon termed desensitization (6). The decrease in TRPV1 activity during desensitization has been shown to be due to a right shift in the capsaicin dose response (7). We and others have shown earlier that activation of TRPV1 leads to activation of a Ca^{2+}-sensitive PLC, most likely a PLCδ isoform (8), which leads to a robust decrease in the levels of $PI(4,5)P_2$ (7, 9, 10). Because $PI(4,5)P_2$ is required for TRPV1 activity, depletion of this lipid is a major factor in desensitization (11). The products of $PI(4,5)P_2$ hydrolysis by PLC are inositol 1,4,5-trisphosphate and DAG. DAG activates PKC; although the role of this enzyme is very well established in sensitization (4, 12, 13), the role of endogenous DAG in desensitization is essentially unexplored.

Here we find that inhibition of DAGK enzymes that phosphorylate DAG leads to diminished desensitization of capsaicin-induced currents of native TRPV1 in DRG neurons and recombinant TRPV1 expressed in HEK293 cells. The effect of DAGK inhibition was eliminated when the two key PKC phosphorylation residues, Ser-502 and Ser-800 (4), were mutated. We also found that activation of TRPV1 induced only a small and transient increase in DAG levels, in contrast to the robust and sustained increase evoked by activation of the G_q-coupled M1 muscarinic receptors. Inhibition of DAGK activity substantially increased DAG accumulation induced by TRPV1 activation but not by muscarinic receptor activation. These data indicate that DAG production upon TRPV1 activation is limited by DAGK activation. Our findings uncover a novel role for DAGK enzymes in regulation of TRPV1 activity.

Results

DAGK inhibition reduces capsaicin-induced desensitization of TRPV1 currents

To examine the role of DAGK enzymes in TRPV1 channel desensitization, we measured inward currents evoked by capsaicin in mouse DRG neurons at −60 mV holding potential, using the whole-cell patch clamp technique. Consistent with earlier results, capsaicin-induced currents decayed substantially after an initial peak during 75-s application of 1 μM capsaicin. When capsaicin was reapplied 3 min later, it evoked smaller currents (Fig. 1*A*) whose amplitudes, on average, were less than 20% of the first peak current (Fig. 1*D*). The decrease in the amplitude of the second application of capsaicin is sometimes referred to as tachyphylaxis to differentiate it from the

* For correspondence: Tibor Rohacs, tibor.rohacs@rutgers.edu.

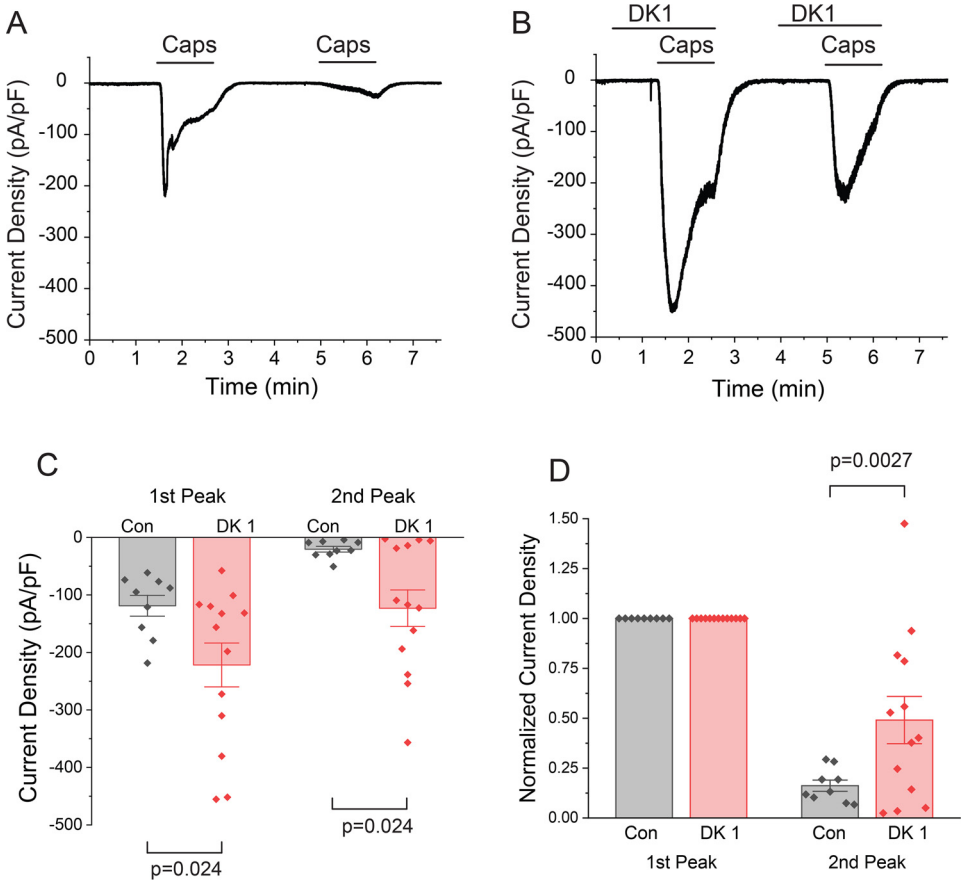

Figure 1. Inhibition of DAGK potentiates TRPV1 channel activity in DRG neurons. *A*, representative whole-cell voltage clamp trace of inward currents recorded at −60 mV from mouse DRG neurons. Measurements were conducted in 2 mM Ca^{2+} EC solution. Capsaicin (*Caps*, 1 μM) was applied to activate TRPV1 channels for 75 s twice, as indicated by the *horizontal lines*. *B*, similar measurement with coapplication of the DK1 (R59022, 50 μM), as indicated by the *horizontal lines*. *C*, statistical analysis of experimental groups for control (*Con*, $n = 9$ neurons) and DK1 ($n = 13$ neurons). Statistical significance was calculated with two-way analysis of variance with Fisher's post hoc test. $F(3,40) = 7.14$, $p = 0.00059$. *pF*, picofarad. *D*, statistical analysis of the same data after currents were normalized to the peak value; two-way analysis of variance, $F(3,40) = 30.5$, $p = 2.0 \times 10^{-10}$. Data are shown as mean ± S.E. and scatterplots.

current decay during the first capsaicin application, which is termed acute desensitization (6). When the neurons were treated with DAGK inhibitor 1 (DK1), also called R59022 (14), the peak amplitude during the first and second capsaicin application became significantly larger (Fig. 1, *B* and *C*). When the current amplitudes were normalized to the first peak in both groups, the relative currents evoked by the second capsaicin application were significantly larger in the DK1-treated group (Fig. 1*D*), indicating reduced tachyphylaxis. DK1, on average, did not alter the kinetics and extent of acute desensitization (data not shown).

Next we tested the involvement of PKC phosphorylation of TRPV1. We transfected HEK293 cells with WT TRPV1 or the S502A/S800A mutant of TRPV1 that lacks the critical phosphorylation sites for PKC-induced sensitization (4). Fig. 2, *A*, *B*, *E*, and *F*, show that, in TRPV1-expressing cells treated with DK1, the peak amplitude of the capsaicin-induced current was higher than in cells not treated with DK1 in the first capsaicin application. The peak current induced by the second capsaicin application showed a more robust increase in DK1-treated cells, and thus the ratio of the second to first peak amplitude increased significantly in cells treated with DK1 (Fig. 2*F*), indicating reduced desensitization (tachyphylaxis). DK1, on the other hand, did not have any effect on the amplitudes of the currents induced by the first or the second capsaicin application in the S502A/S800A mutant of TRPV1 (Fig. 2, *C–E*). Fig. 2, *G* and *H*, shows that, when the current amplitudes were normalized to the peak of the first capsaicin application in each group, DK1, on average, slowed the current decay (acute desensitization) in cells transfected with the WT TRPV1 but not in cells expressing the S502A/S800A mutant. Overall, these data show that DK1 reduces capsaicin-induced desensitization of TRPV1 in a PKC phosphorylation–dependent manner.

DAGK inhibition potentiates DAG accumulation in response to TRPV1 activation

The effect of the DAGK inhibitor DK1 suggests that DAG accumulation is limited by DAGK activity in response to capsaicin. To test this, next we measured cellular DAG signals using fluorescent sensors in response to TRPV1 stimulation. First, we transfected HEK293 cells with a green fluorescent DAG sensor that responds with an increase in fluorescence intensity to DAG formation, a red fluorescent Ca^{2+} sensor (Red-GECO) (15), as well as TRPV1 and muscarinic M1 receptors to measure cytoplasmic Ca^{2+} levels simultaneously with DAG levels. Fig. 3*A* shows that activation of the G_q-coupled M1 receptors by carbachol induced a large increase in DAG and cytoplasmic Ca^{2+} levels in these cells. When capsaicin was

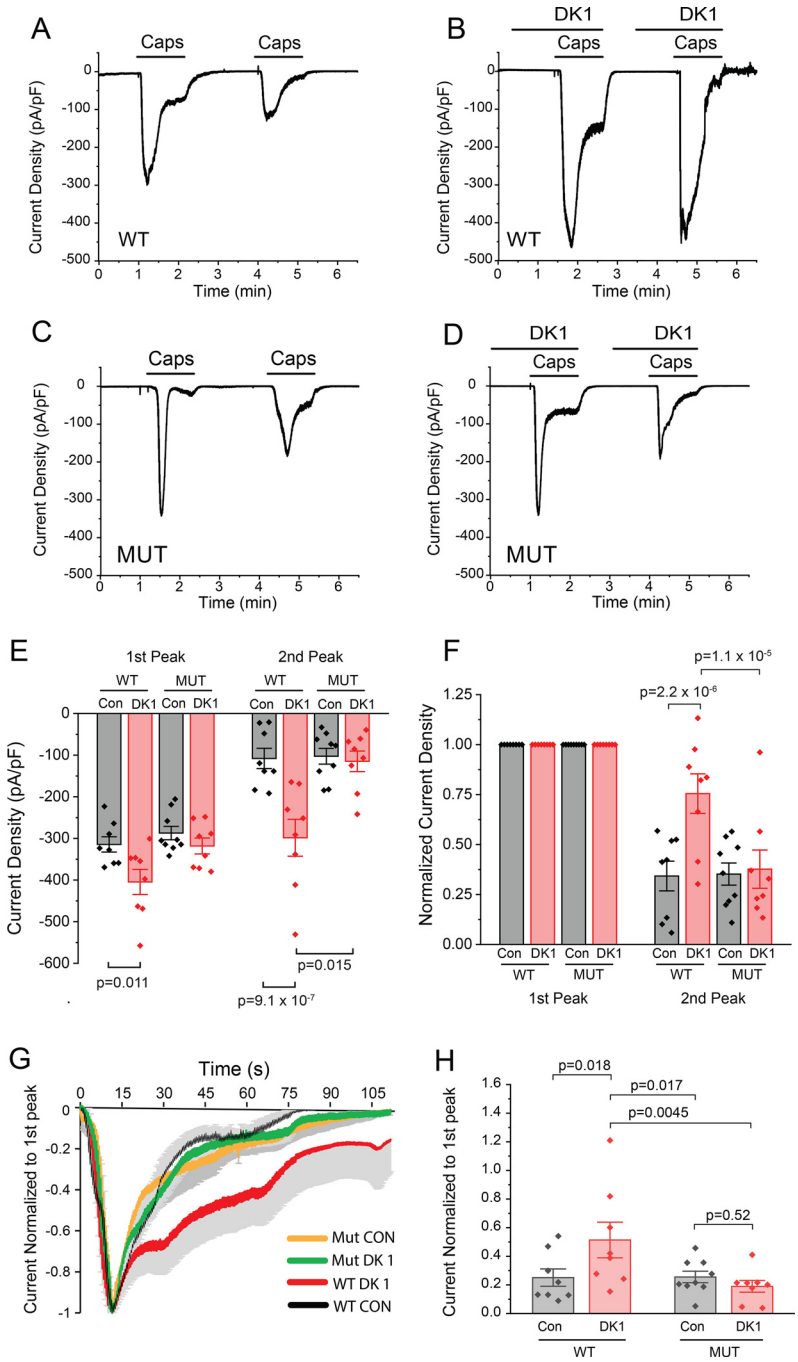

Figure 2. Inhibition of diacylglycerol kinases potentiates TRPV1 activity and reduces desensitization in a PKC-dependent manner. *A–D*, representative whole-cell voltage clamp traces of inward currents recorded at −60 mV from HEK293 cells transfected with WT TRPV1 or the PKC phosphorylation–deficient S502A/S800A double mutant (*MUT*) TRPV1. Measurements were conducted in 2 mM Ca^{2+} EC solution. Capsaicin (*Caps*, 1 μM) was applied to activate TRPV1 channels for 75 s twice, as indicated by *short horizontal lines*. Applications of 50 μM DK1 are indicated by *longer horizontal lines*. *pF*, picofarad. *E*, statistical analysis for WT control ($n = 8$), WT DK1 ($n = 8$), mutant control (*Con*, $n = 9$), and mutant DK1 ($n = 8$). Statistical significance was calculated with three-way analysis of variance; $F(11,54) = 12.45$, $p = 2.97 \times 10^{-11}$; Fisher's post hoc test was used to calculate *p* values. *F*, statistical analysis of the same data with currents normalized to the first peak value; two-way analysis of variance. $F(11,54) = 18.1$, $p = 2.1 \times 10^{-14}$. *G*, normalized currents (mean ± S.E.) during the first application of capsaicin. *H*, statistical analysis 35 s after the first peak current; two-way analysis of variance. $F(3,29) = 3.77$, $p = 0.021$. Data in *E*, *F*, and *H* are shown as mean ± S.E. and scatterplots.

applied after carbachol, it evoked an increase in Ca^{2+} but a decrease in fluorescence of the DAG sensor. When capsaicin was applied first, it induced a clear increase in cytoplasmic Ca^{2+} and a decrease in fluorescence of the DAG sensor, preceded by a small transient increase (Fig. 3*B*). Carbachol applied after capsaicin did not induce any Ca^{2+} signal or DAG signal (Fig. 3*B*). We also found that capsaicin induced a large decrease in $PI(4,5)P_2$ levels, indicating PLC activation (Fig. 3, *E–G*), which is consistent with previous publications (9, 10). This decrease in $PI(4,5)P_2$ levels eliminates the substrate for PLC and thus explains why carbachol did not induce any DAG or Ca^{2+} signal after capsaicin.

Next we tested whether DAGK inhibition can rescue the DAG signal in response to TRPV1 activation. Fig. 4, *A* and *B*,

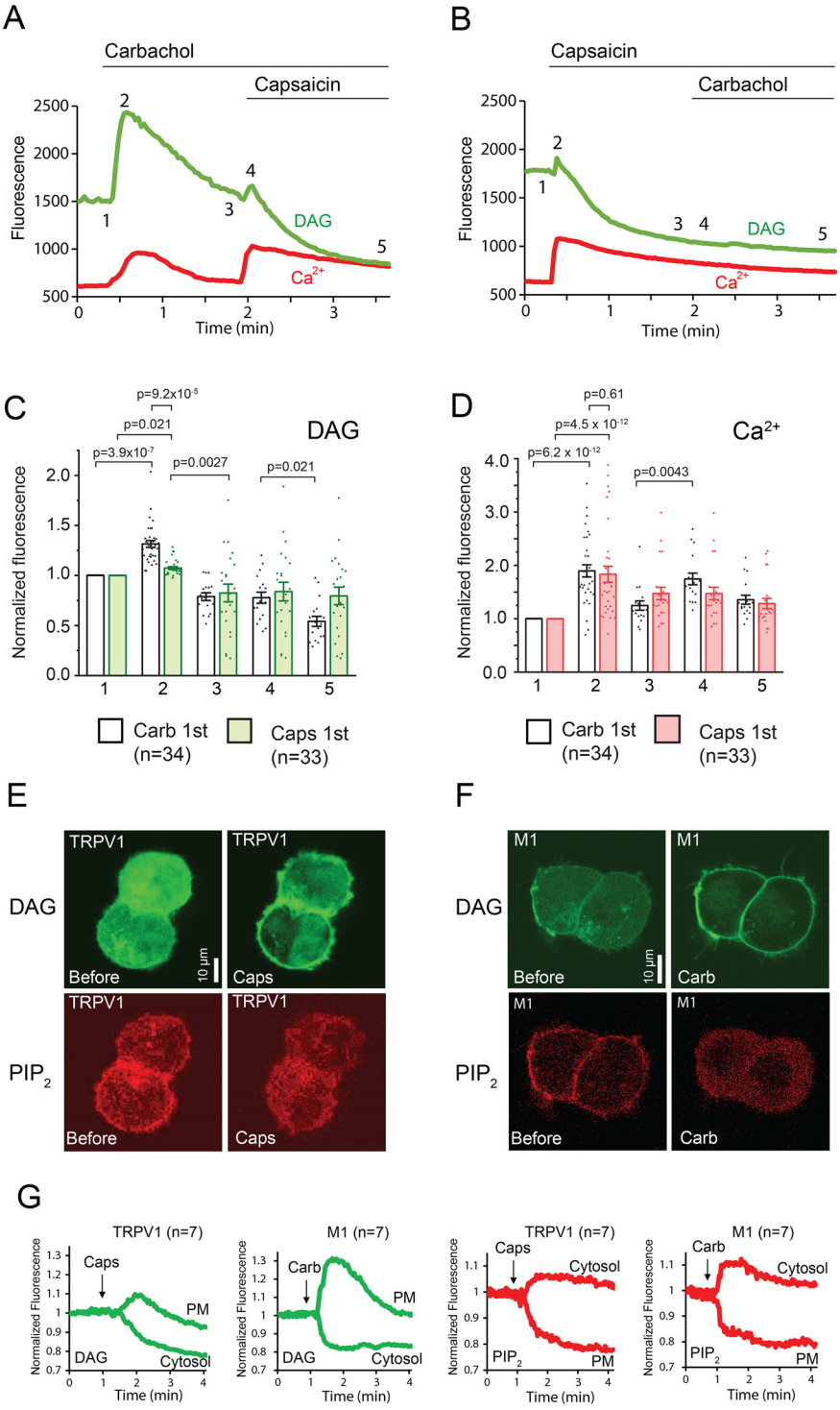

Figure 3. TRPV1 activation induces a transient increase in DAG levels, an increase in cytoplasmic Ca^{2+} levels, and a decrease in plasma membrane $PI(4,5)P_2$ levels. *A* and *B*, representative green and red fluorescence traces of HEK293 cells transfected with the Green-up (DAG)/Red-GECO (Ca^{2+}) sensor, TRPV1, and M1 muscarinic receptors. Carbachol (100 μM) and capsaicin (1 μM) were applied as indicated by the *horizontal lines*. *C* and *D*, statistical analysis of experimental groups for carbachol (*Carb*) first ($n = 34$) and capsaicin (*Caps*) first ($n = 33$) at time points 1, 2, 3, 4, and 5 (as indicated in *A* and *B*). Data are shown as mean ± S.E. and scatterplots. Statistical significance was calculated with two-way analysis of variance; *p* values were calculated with Fisher's post hoc test. $F(9,240) = 18.4$, $p = 3.6 \times 10^{-23}$ (*C*) and $F(9,240) = 3.82$, $p = 4.7 \times 10^{-4}$ (*D*). *E*, representative confocal images of HEK293 cells transfected with TRPV1 + PKDc1ab-GFP (DAG sensor) and PLCPHδ-RFP ($PI(4,5)P_2$ sensor) before and after application of 1 μM capsaicin. *F*, representative confocal images of HEK293 cells transfected with M1 muscarinic receptors and PKDc1ab-GFP and PLCPHδ-RFP before and after application of 100 μM carbachol. *G*, averaged traces of normalized green and red fluorescence intensity in the plasma membrane and cytosol in experimental groups of TRPV1 ($n = 7$) and M1 ($n = 7$).

shows that, in cells treated with DK1, the DAG signal in response to capsaicin was larger than without the inhibitor. The effect of capsaicin on the peak of the DAG signal in the presence of DK1 was not statistically significantly different from that induced by M1 activation by carbachol. DK1 also potentiated the Ca^{2+} responses to capsaicin (Fig. 4, *A* and *C*), which is

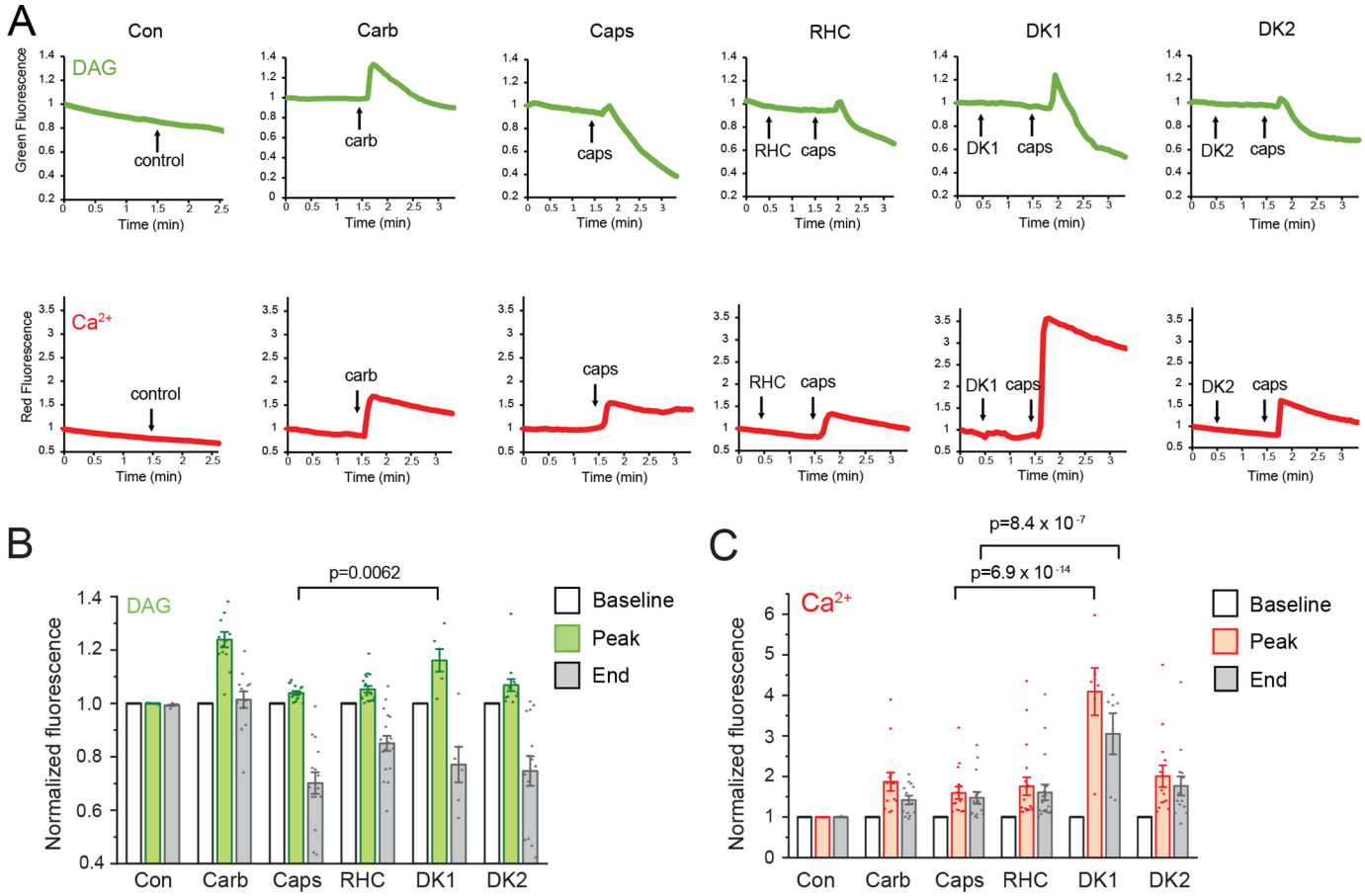

Figure 4. DK1 transiently rescues DAG levels. *A*, HEK293 cells were transfected with Green-up (DAG)/Red-GECO(Ca^{2+}) sensors and either TRPV1 or M1 muscarinic receptors. TRPV1 expressing cells were stimulated with capsaicin (*caps*), M1 expressing cells with carbachol (*carb*). Shown are representative time courses of normalized green (DAG) and red (Ca^{2+}) fluorescence signals upon application of 100 μM carbachol or 1 μM capsaicin with or without 1-min preapplication of the DAGL inhibitor RHC80267 (*RHC*, 50 μM) or the DAGK inhibitors DK1 (50 μM) or DK2 (50 μM), respectively. *Con*, control. *B* and *C*, statistical analysis of baseline, peak, and end of application of capsaicin or carbachol. *B*, normalized green fluorescence for DAG level changes. *C*, normalized red fluorescence for Ca^{2+} level changes. Data are shown as mean ± S.E. and scatterplots. Statistical significance was calculated with two-way analysis of variance and Fisher's post hoc test; $F(17,210) = 27.0$, $p = 1.3 \times 10^{-43}$ (*B*); $F(17,210) = 12.3$, $p = 2.3 \times 10^{-23}$ (*C*).

consistent with its effect on TRPV1 desensitization (Figs. 1 and 2). Pretreatment with DAG kinase inhibitor 2 (DK2; R59949) (14) or the DAG lipase (DAGL) inhibitor RHC80267 (16), on the other hand, had no effect on DAG or Ca^{2+} signals induced by capsaicin (Fig. 4, *A–C*).

Our data show that, without DAG Kinase inhibition, capsaicin induced a negligible DAG signal (Figs. 3*B* and 4*A*), despite clear PI(4,5)P_2 hydrolysis (Fig. 3, *E–G*). Next we tested whether this apparent lack of DAG accumulation was due to the low affinity of the DAG sensor we used. To this end, we transfected HEK293 cells with the high-affinity DAG sensor containing the tandem C1 domains (C1ab) of protein kinase D1 fused to the C terminus of GFP (GFP-PKD C1ab) as well as TRPV1 and M1 muscarinic receptors (17). The GFP-PKD C1ab sensor translocates from the cytoplasm to the plasma membrane in response to an increase in DAG concentration, which we monitored using confocal microscopy. We found that, in response to capsaicin, this sensor displayed clear translocation to the plasma membrane (Fig. 5, *A* and *C*), but the effect was smaller and more transient than the translocation induced by carbachol (Fig. 5, *B* and *D*). TRPV1 activation by capsaicin also prevented carbachol from inducing a DAG signal (Fig. 5*A*). In cells pretreated with DK1, capsaicin induced a more sustained DAG signal than in the absence of the inhibitor (Fig. 5, *A* and *C*), but DK1 had no effect on the translocation induced by carbachol (Fig. 5, *B* and *D*). The DAG signal induced by capsaicin in the presence of DK1 was comparable with that induced by carbachol (Fig. 5, *C* and *D*).

Our data indicate that DAGK, but not DAGL activity, decreases DAG accumulation in response to TRPV1 activation. To confirm this conclusion, we used additional pharmacological tools: the DAGK inhibitor ritanserin (18) and the DAGL inhibitor DO34 (19). Fig. 6, *A–C*, shows that the transient DAG signal induced by TRPV1 activation became sustained in cells treated with ritanserin but not in cells treated with DO34.

PKC inhibition accelerates capsaicin-induced acute desensitization, but not tachyphylaxis, in DRG neurons

Our data with the two different DAG sensors show that TRPV1 activation induces a DAG signal even though it is transient and smaller than that induced by muscarinic receptor activation. Next, we tested whether this small transient increase in DAG has any effect on desensitization. We measured capsaicin-induced inward currents in DRG neurons in the presence

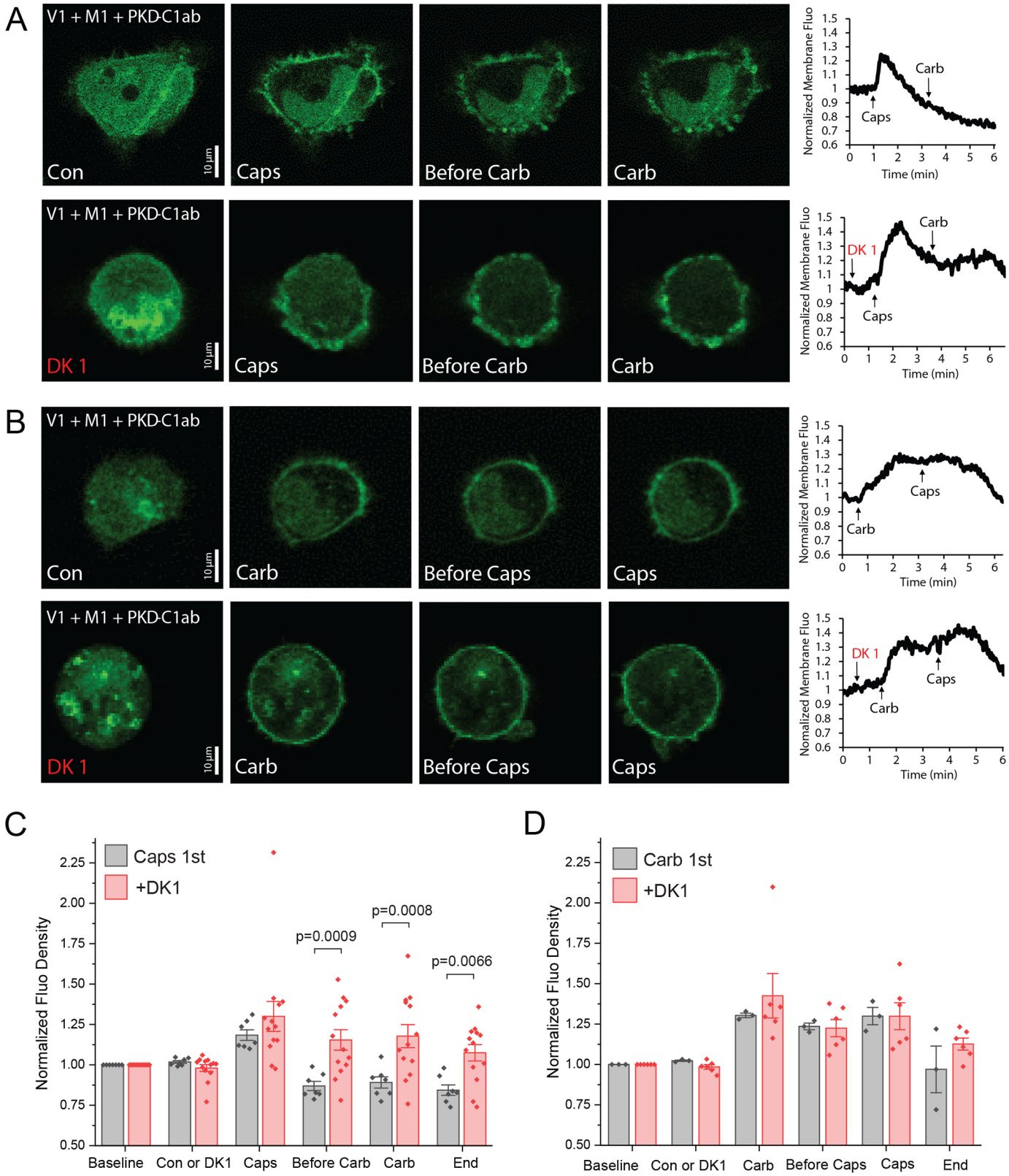

Figure 5. Application of DK1 increases DAG levels upon capsaicin-induced TRPV1 activation. *A* and *B*, representative confocal fluorescence images of HEK293 cells transfected with the high-affinity PKDc1ab-GFP (DAG) sensor, TRPV1, and M1 with or without 1-min preapplication of DK1 (*top* and *bottom rows*, respectively). Time courses of fluorescence changes (normalized to baseline) in the plasma membrane are shown on the *right* next to the representative images for each cell. *A*, cells were stimulated by 1 μM capsaicin (*Caps*), followed by 100 μM carbachol (*Carb*). *Con*, control. *B*, cells were first stimulated by 100 μM carbachol, followed by 1 μM capsaicin. *C*, statistical analysis of cells first stimulated by capsaicin in the control group (*black*, $n = 7$) and in the DK1 group (*red*, $n = 13$). *D*, statistical analysis of cells first stimulated by carbachol in the control group (*black*, $n = 3$) and DK1 group (*red*, $n = 6$). Data are shown as mean ± S.E. and scatterplots. Statistical significance was calculated with two-way analysis of variance with Fisher's post hoc test; $F(11, 108) = 6.05$, $p = 1.23 \times 10^{-7}$ (*C*); $F(11, 41) = 4.59$, $p = 0.00016$ (*D*).

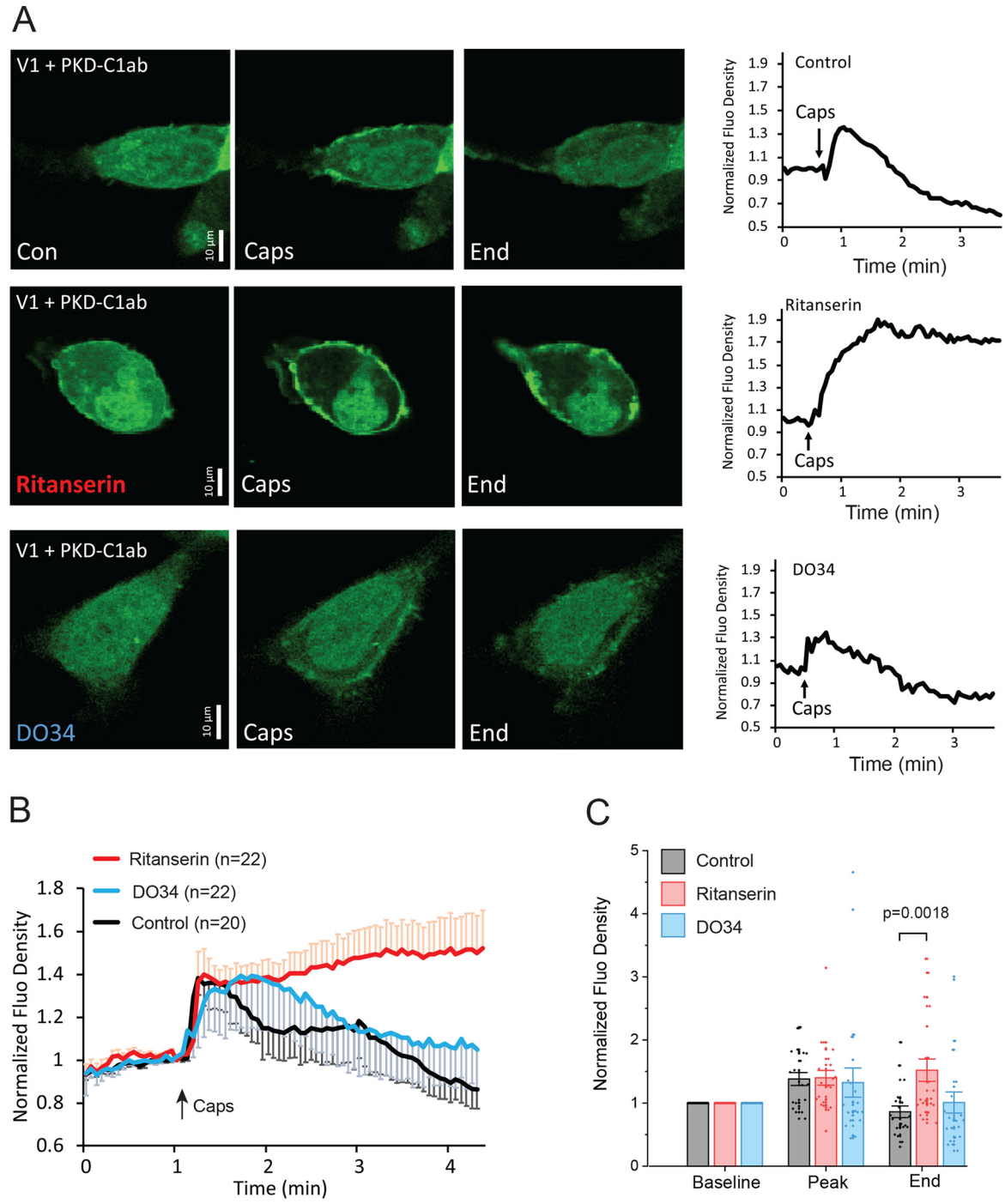

Figure 6. The DAG kinase inhibitor ritanserin, but not the DAGL inhibitor DO34, increases DAG levels upon capsaicin-induced TRPV1 activation. *A*, representative confocal fluorescence images of HEK293 cells transfected with the high-affinity PKDc1ab-GFP (DAG) sensor and TRPV1 before the application of 1 μM capsaicin (*Con*, control, *left column*) at the maximal effect (*Caps, center column*), and 3 min after application of capsaicin (*End, right column*). The *top row* shows control experiments. The *center row* shows 1-min pretreatment with the DAGK inhibitor ritanserin (50 μM). The *bottom row* shows the effect of 1-min pretreatment with the DAGL inhibitor DO34 (1 μM). Time courses of fluorescence changes (normalized to baseline) in the plasma membrane are shown on the right next to the representative images for each cell. *B*, time course of the mean ± S.E. of plasma membrane fluorescence. *C*, bar graphs (mean ± S.E.) and scatterplots for normalized plasma membrane fluorescence. Statistical significance was calculated with two-way analysis of variance and Fisher's post hoc test; $F(11, 240) = 3.51$, $p = 0.00014$.

and absence of two different PKC inhibitors (Fig. 7, *A–F*). We found that neither bisindolylmaleimide IV (BIM-IV) nor Gö6976 had a significant effect on the peak current amplitudes evoked by two consecutive 1-min applications of 1 μM capsaicin (Fig. 7, *A–D*). BIM-IV pretreatment accelerated the current decay during the initial phase of the first capsaicin application (acute desensitization) (Fig. 7, *A*, *C*, *E*, and *F*). Gö6976, on the other hand, induced only a marginal effect on acute desensitization (Fig. 7, *A*, *B*, *E*, and *F*), which did not reach statistical significance. This is consistent with Gö6976 not inhibiting PKCε (20), the isoform that plays a major role in TRPV1 phosphorylation (12). Neither BIM-IV nor Gö6976 had an effect on the peak amplitude (Fig. 7*D*) or the decay kinetics (data not shown) of the second capsaicin application.

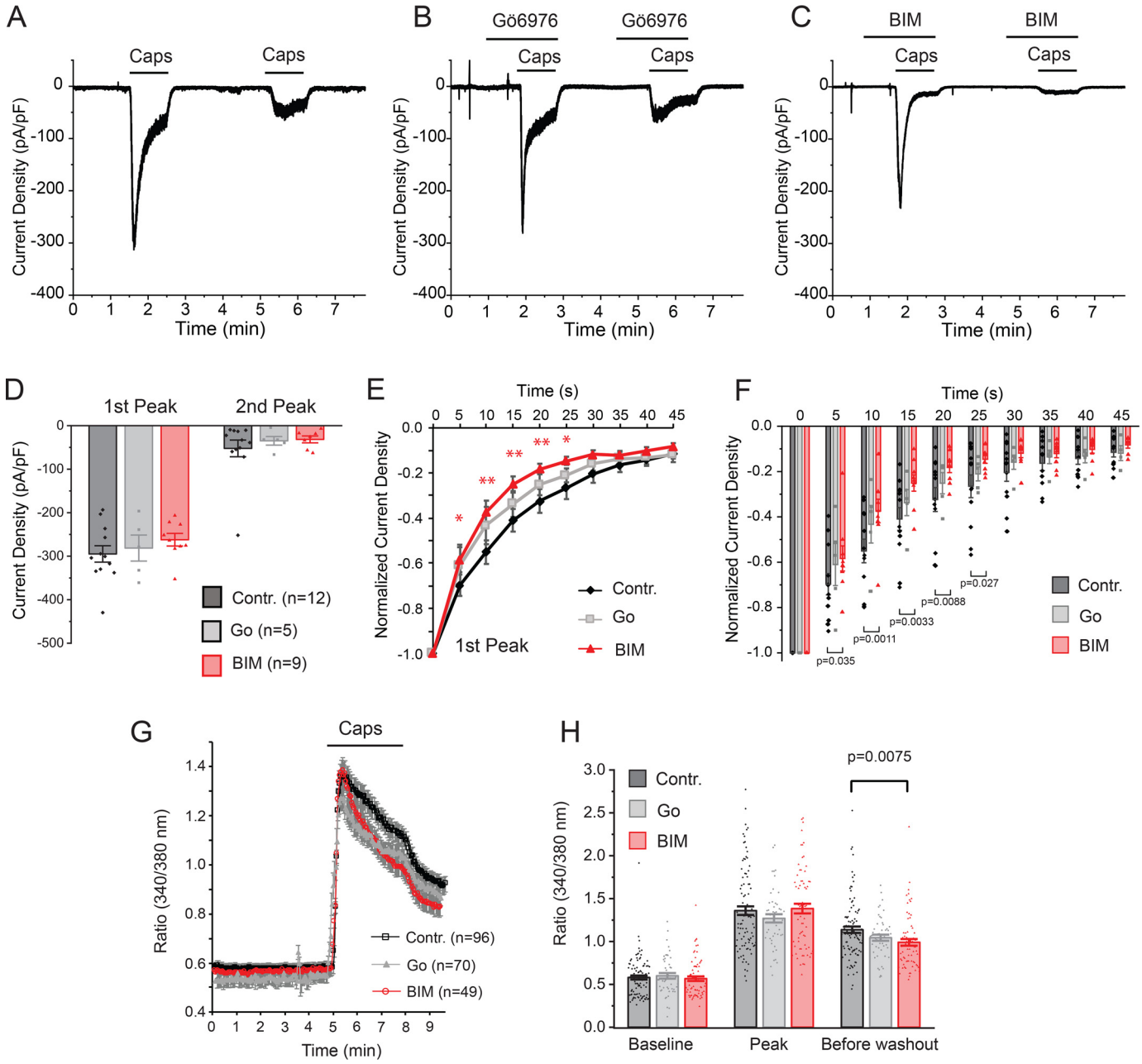

Figure 7. PKC inhibition accelerates acute desensitization of TRPV1 in DRG neurons. *A–C*, representative whole-cell voltage clamp traces of inward currents recorded at −60 mV from DRG neurons. Measurements were conducted in 2 mM Ca^{2+} EC solution. Capsaicin (*Caps*, 1 μM) was applied to activate TRPV1 channels for 1 min twice, as indicated by the *horizontal lines*. Control: no PKC inhibitor preapplication (*A*), 2 μM Gö6976 preapplication for 1 min (*B*), and 1 μM BIM-IV (*BIM*) preapplication for 1 min (*C*). *pF*, picofarad. *D*, summary of peak current amplitudes induced by the first and second applications of capsaicin. *E* and *F*, statistical analysis of current decay of capsaicin-induced current during the first application normalized to the peak amplitudes; points show mean ± S.E. (*E*) and scatterplots (*F*). Statistical significance was calculated with two-way analysis of variance and Fisher's post hoc test; $F(29, 224) = 45.5$, $p = 7.34 \times 10^{-78}$. The *asterisks* in *E* indicate a difference between the BIM-treated group and control, and they correspond to the *p* values in *F*. *G*, averaged traces (± S.E.) of Ca^{2+} imaging data in DRG neurons loaded with the low-affinity Ca^{2+} sensor Fura-2FF upon stimulation of capsaicin with or without 1 min preapplication of 1 μM BIM-IV or 2 μM Gö6976. *H*, statistical analysis of *G* at baseline, peak after capsaicin application, and before washout of capsaicin. Data are shown as mean ± S.E. and scatterplots. Statistical significance was calculated with two-way analysis of variance with Fisher's post hoc test; $F(8, 636) = 67.8$, $p = 3.5 \times 10^{-80}$.

The small effect of PKC limited to the initial phase of acute desensitization is consistent with the transient DAG signal in response to capsaicin (Fig. 5). In agreement with the patch clamp experiments, in DRG neurons loaded with the low-affinity Ca^{2+} indicator FuraFF, the Ca^{2+} response to 1 μM capsaicin became more transient in the presence of BIM-IV but not Gö6976 (Fig. 7, *G* and *H*).

Overall, our data show that DAGK activation reduces DAG accumulation in response to TRPV1 activation, which limits the role of PKC to modulating the initial phase of acute desensitization. Fig. 8 shows our overall model of the involvement of DAGK and PKC in TRPV1 regulation during desensitization.

Discussion

The sensitivity of TRPV1 to capsaicin and other stimuli is not static. Upon activation of G_q-coupled receptors, the channel becomes more sensitive to capsaicin, which manifests as a left shift in the capsaicin concentration response relationship but

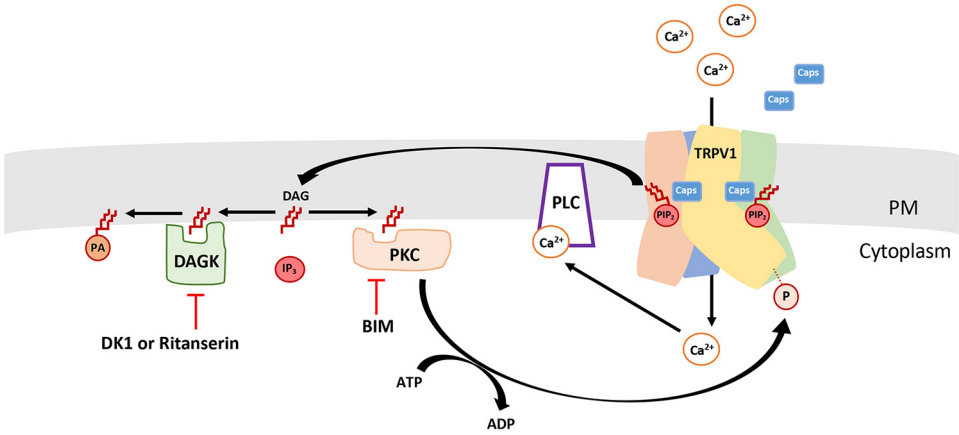

Figure 8. Cartoon explaining the role of DAGK and PKC in the regulation of TRPV1.

no change in the maximal response (3). This increased sensitivity is largely mediated by direct phosphorylation of the channel by PKC at residues Ser-502 and Ser-800 (4). When the channel is activated by high concentrations of capsaicin, channel activity desensitizes (6), which manifests as a right shift in the capsaicin concentration–response curve (7). It has been shown that Ca^{2+} influx via TRPV1 activates a Ca^{2+} sensitive PLC, which leads to depletion of $PI(4,5)P_2$ (7, 8, 10), and that loss of this lipid is an important factor in desensitization (11). Although it has been shown that pharmacological activation of PKC with phorbol 12-myristate 13-acetate slows desensitization (21, 22), it is not known whether endogenous DAG and consequential PKC activation modulate desensitization. Here we found that, despite robust PLC activation, TRPV1 stimulation leads to only a small and transient increase in DAG levels as opposed to the robust DAG signal induced by activation of G_q-coupled M1 muscarinic receptors. The DAG signal induced by TRPV1 activation was potentiated by DAGK inhibition, indicating that DAGK activity limited DAG accumulation. DAGK inhibition, on the other hand, had no effect on the DAG signal induced by activation of G_q-coupled M1 receptors. Consistent with positive regulation of TRPV1 by PKC, DAGK inhibition also reduced capsaicin-induced desensitization of TRPV1 in a PKC-dependent manner.

We used two different sensors of DAG in this study. The first sensor is based on a circularly permutated GFP placed between the pseudosubstrate domain and the DAG binding C1 domain of PKCδ (23) and responds with an increase in fluorescence in response to G_q-coupled receptor stimulation and phorbol esters (15). In our experiments, this sensor showed only a very small and transient increase in DAG levels in response to TRPV1 activation, whereas it showed a robust but still transient increase to M1 muscarinic receptor activation (Figs. 3 and 4). The high-affinity GFP-PKD C1ab DAG probe has been shown to translocate to the plasma membrane in response to G_q-coupled receptor stimulation, application of diC_8 DAG, and phorbol esters (17). The GFP-PKD C1ab probe detected a clear increase in DAG levels in response to TRPV1 activation, which was smaller and more transient than that induced by muscarinic receptor activation (Fig. 5). In both cases, treating the cells with the DAGK inhibitor DK1 increased the DAG signal evoked by TRPV1 activation. This indicates that DAG is generated when TRPV1 is activated but that its levels are diminished by DAGK activation, making the signal small and transient.

We studied TRPV1 desensitization using two consecutive capsaicin applications. During the first application of capsaicin, current levels decreased substantially despite the continuous presence of capsaicin; this decrease is often referred to as acute desensitization. The peak amplitude of the second capsaicin application is a lot smaller than that of the first one; this decrease in the response to the second application is sometimes referred to as tachyphylaxis. Although depletion of $PI(4,5)P_2$ plays a crucial role in these phenomena (8, 10), in this study, we found different effects on acute desensitization and tachyphylaxis when we pharmacologically modified the PKC pathway at two different targets. The DAGK inhibitor DK1 had a more robust effect on tachyphylaxis (Figs. 1 and 2); the PKC inhibitor BIM-IV, on the other hand, only affected acute desensitization (Fig. 7). These data are consistent with our measurements showing that DAG formation in response to capsaicin is transient, which explains why the PKC inhibitor BIM-IV only affected the early phase of acute desensitization. The presence of a DAGK inhibitor, on the other hand, allows increased DAG levels at both capsaicin applications, explaining why tachyphylaxis was affected. Overall, we conclude that rapid phosphorylation of DAG by DAGK limits the role of PKC to a small effect during the initial phase of acute desensitization of TRPV1.

Interestingly, pretreatment with DK1 also increased the amplitude of the peak current evoked by the first capsaicin application in DRG neurons (Fig. 1) and in HEK cells (Fig. 2), and this effect was more pronounced in DRG neurons. A potential explanation for this is the following. With the relatively slow whole-chamber perfusion system in our patch clamp experiments, even during the upstroke of the current, some desensitization may occur, limiting the maximum macroscopic current. The increased DAG formation in DK1-treated cells could counteract this process, leading to an increase in peak amplitude. It has been shown that components of desensitization and sensitization, including PKC, are anchored to TRPV1 by the scaffolding protein AKAP79/150, making such fast signaling possible (13).

DAG formed upon PLC activation can be metabolized by DAGK enzymes that phosphorylate DAG and generate phosphatidic acid and DAGL enzymes that remove one acyl chain, leading to formation of 2-arachidonylglycerol (2-AG) (24). We

found that inhibition of DAGK by DK1 and ritanserin potentiated the DAG signal evoked by TRPV1 activation, indicating that DAGK limited DAG accumulation. Inhibition of DAGL enzymes using RHC80267 or DO34, on the other hand, did not influence the DAG signal, indicating that DAGL enzymes do not play a role in metabolizing DAG generated in response to TRPV1 activation. DAG can also potentially be converted to triacylglycerol by DAG acyltransferase enzymes (25); exploring their role in TRPV1 regulation will require further studies.

There are 10 isoforms of DAGK in mammals, divided into five different groups based on the presence of conserved domains (26). Type 1 enzymes (α, β, and γ) are activated by Ca^{2+}; therefore, they are potential candidates for the isoenzymes activated by TRPV1 activation. These isoforms, however, are inhibited similarly by DK1 and DK2 (14, 27), and our finding that DK1, but not DK2, potentiated DAG formation by TRPV1 activation argues against involvement of these isoforms. An additional argument against involvement of Ca^{2+}-sensitive DAGK isoforms is the finding that the DAG signal induced by M1 muscarinic receptor activation was not potentiated by DK1 (Fig. 5*B*) despite carbachol inducing a Ca^{2+} signal similar to that induced by capsaicin (Fig. 4*C*).

Ritanserin was originally described as a serotonin receptor antagonist; it is structurally similar to DK1, and it has been shown to inhibit DAGKα (18), but there is no information on the effect of this compound on other DAGK isoforms. Similar to DK1, ritanserin also potentiated the DAG signal evoked by TRPV1 activation.

It has been reported that DAGKϵ and DAGKθ are inhibited by DK1 but not by DK2 (14), raising the possibility that these isoforms are responsible for the effect of DK1 in our study. The literature regarding the selectivity of these inhibitors, however, is conflicting; inhibition of DAGKθ by DK1 was confirmed by Tu-Sekine *et al.* (28) but contested by Boroda *et al.* (18). Another report showed that DK2 also inhibits DAGKθ (29). Thus, it is hard to draw firm conclusion regarding the selectivity of DK1 and DK2 on DAGKθ.

Given the reported differential of effect of DK1 and DK2 on DAGKϵ (14) and the differential of effect of DK1 and DK2 on DAG production induced by TRPV1 activation (Fig. 4), DAGKϵ is a potential candidate for involvement in TRPV1 regulation. This isoform is highly specific for arachidonyl-stearyl DAG (30, 31), which is the dominant lipid formed by PLC activation. $PI(4,5)P_2$ has been reported to inhibit DAGKϵ with very high affinity (32, 33). PI(4)P, the precursor of $PI(4,5)P_2$, also inhibits DAGKϵ, but it is less potent than $PI(4,5)P_2$ (32). We found earlier that TRPV1 activation induces a more robust decrease in $PI(4,5)P_2$ and PI(4)P levels than that evoked by G_q-coupled receptor activation (8, 9). Relief from inhibition by $PI(4,5)P_2$ and PI(4)P thus gives a potential mechanism for activation of DAGKϵ. DAGKϵ is also potentiated by Ca^{2+} (33), giving an additional mechanism for its stimulation by TRPV1 activation. Overall, however, the large number of DAGK isoforms and their conflicting pharmacological characterization makes it beyond the scope of this study to identify the DAGK isoform involved in TRPV1 regulation.

Relatively little is known about the role of DAGK enzymes in ion channel regulation. For the $PI(4,5)P_2$-dependent KCNQ2/3, channel it has been reported that DAGK or DAGL inhibition had no effect on channel inhibition by muscarinic receptor activation (34). In *Drosophila* photoreceptors, mutation of the rgda gene that encodes a DAGK induces retinal degeneration and constitutive activity of the DAG-sensitive TRP channels (35). Our work uncovers a novel role of DAGK in the regulation of the heat- and capsaicin-activated TRPV1 channels.

Experimental procedures

DRG neuron isolation and preparation

All animal procedures were approved by the Institutional Animal Care and Use Committee at Rutgers New Jersey Medical School. DRG neurons were isolated from 3- to 6-month-old C57BL6 mice. DRG neurons were isolated from mice of either sex and anesthetized with i.p. injection of ketamine (100 mg/kg) and xylazine (12 mg/kg). The detailed methods for DRG neuron isolation and digestion have been described previously (36). After digestion with 3 mg/ml type I collagenase (Worthington) and 5 mg/ml dispase, neurons were seeded onto glass coverslips coated with a mixture of poly-D-lysine (Invitrogen) and laminin (Sigma). Neurons were then cultured for 16–48 h before measurements in DMEM–F12 supplemented with 10% FBS (Thermo Scientific), 100 IU/ml penicillin, and 100 μg/ml streptomycin in a humidity-controlled tissue culture incubator maintaining 5% CO_2 at 37 °C.

HEK293 cell culture and preparation

HEK293 cells were obtained from the ATCC (catalog no. CRL-1573) and cultured in minimal essential medium (Invitrogen) containing supplements of 10% (v/v) Hyclone-characterized FBS (Thermo Scientific), 100 IU/ml penicillin, and 100 μg/ml streptomycin. Transient transfection was performed at ~70% cell confluence using Effectene reagent (Qiagen) according to the manufacturer's protocol. After transfection, cells were incubated overnight (16–20 h) with transfection reagents containing the lipid–DNA complexes. Then the cells were trypsinized and replated on to poly-D-lysine–coated glass coverslips and cultured at least for an additional 2 h (in the absence of the transfection reagent) before measurements in a humidity-controlled tissue culture incubator maintaining 5% CO_2 at 37 °C. The complementary DNA used for transfecting HEK293 cells was prepared using the Endo-Free Plasmid Maxi Kit from Qiagen. The WT rat TRPV1 clone was provided by Dr. David Julius (University of California San Francisco). The S502A/S800A TRPV1 mutant was from Dr. Makoto Tominaga (National Institute for Physiological Sciences). The Green-up (DAG)/Red-GECO (Ca^{2+}) sensor was from Dr. Thomas Hughes (Montana State University). The PKDc1ab-GFP DAG sensor and PLCPHδ-RFP $PI(4,5)P_2$ sensor were from Dr. Tamas Balla (National Institutes of Health).

Electrophysiology

Whole-cell patch clamp recordings were performed at room temperature. Patch pipettes were pulled from borosilicate glass capillaries (1.75 mm outer diameter, Sutter Instruments) on a P-97 pipette puller (Sutter Instrument) to a resistance of 4–6 megaohm. After formation of the gigaohm seal, the whole-cell configuration was established, and currents were measured at a holding potential of −60 mV for DRG neurons and HEK293

cells using an Axopatch 200B amplifier (Molecular Devices). Currents were filtered at 2 kHz using the low-pass Bessel filter of the amplifier and digitized using a Digidata 1440 unit (Molecular Devices). Recordings were conducted using the Clampex software, and data analysis was performed using Clampfit software (Molecular Devices).

Measurements were conducted in solutions based on Ca^{2+} containing extracellular (EC) medium consisting of 137 mM NaCl, 5 mM KCl, 1 mM $MgCl_2$, 10 mM HEPES, 10 mM glucose, and 2 mM $CaCl_2$ (pH adjusted to 7.4 with NaOH) (8). Intracellular solutions for DRG measurements consisted of 130 mM K-gluconate, 10 mM KCl, 2 mM $MgCl_2$, 2 mM Na_2ATP, 0.2 mM Na_2GTP, 1.5 mM $CaCl_2$, 2.5 mM EGTA, and 10 mM HEPES (pH adjusted to 7.25 with KOH). Intracellular solutions for HEK293 whole-cell measurements consisted of 130 mM KCl, 10 mM KOH, 3 mM $MgCl_2$, 2 mM Na_2ATP, 0.2 mM Na_2GTP, 0.2 mM $CaCl_2$, 2.5 mM EGTA, and 10 mM HEPES (pH adjusted to 7.25 with KOH) (8). Carbachol (carbamoylcholine chloride), DK1 (R59022), DK2 (R59949), and the DAG lipase inhibitor RHC80267 and ritanserin were purchased from Sigma-Aldrich. BIM-IV was from Santa Cruz Biotechnology (Dallas, TX, USA). Gö6976 was purchased from Abcam and DO43 from Aobious Inc. Solutions were applied using a gravity-driven whole-chamber perfusion system.

Ca^{2+} imaging

Ca^{2+} imaging measurements were performed on an Olympus IX-51 inverted microscope equipped with a DeltaRAM excitation light source (Photon Technology International). DRG neurons were loaded with 1 μM low-affinity Fura-2FF/AM (Invitrogen) for 50 min in Ca^{2+} containing EC solution supplemented with 0.1 mg/ml bovine serum albumin before the measurement at room temperature. Images at 340-nm and 380-nm excitation wavelengths were recorded with a Roper Cool-Snap digital CCD (charge coupled device) camera using a ×20 objective; the emission wavelength was 510 nm. Measurements were conducted in Ca^{2+}-containing (EC) solution (8). Cells were analyzed for increases or decreases in fluorescence intensity of the whole cell. Image analysis was performed using Image Master software (PTI). Drugs were applied using a gravity-driven whole-chamber perfusion system.

Confocal fluorescence imaging

Confocal measurements were conducted with an Olympus FluoView-1000 confocal microscope in the frame scan mode using a ×60 water immersion objective at room temperature (~25 °C). Green fluorescence was measured using an excitation wavelength of 473 nm; emission was detected through a 515/50-nm band-pass filter. Red fluorescence was measured using an excitation wavelength of 559 nm; emission was detected through a 585/50-nm band-pass filter. Image analysis was performed using Olympus FluoView-1000 and ImageJ. Measurements were performed in the same extracellular solution as used for electrophysiology. Drugs were directly applied to the experimental chamber, followed by gentle mixing.

Wide-field fluorescence imaging

Wide-field fluorescence measurements were performed on an Olympus IX-81 inverted microscope equipped with an ORCA-FLASH 4.0 camera (Hamamatsu) using a ×40 oil immersion objective. Cells were imaged live at room temperature. To detect the green fluorescence from the Green-up DAG sensor, we used 480 ± 15 nm excitation and 535 ± 20 nm emission filters. Red-GECO Ca^{2+} sensor fluorescence was detected with 575 ± 25 nm and 640 ± 25 nm excitation and emission filters. For simultaneous imaging, the motorized filter turret was utilized to switch filter cubes between measuring the green and red fluorescence. Cells were analyzed for increases or decreases in fluorescence intensity of the whole cell. Data were analyzed using the Metamorph and Image J softwares. Measurements were performed in the same extracellular solution as used for electrophysiology. Drugs were directly applied to the experimental chamber, followed by gentle mixing.

Data analysis and statistics

Data analysis was performed in Excel and Microcal Origin. Data collection was randomized. Data were plotted as mean ± S.E. and scatter plots for most experiments. Data were analyzed with analysis of variance with Fisher's post hoc test. The results of the analyses of variance are reported in the figure legends.

Data availability

All data are contained within the manuscript.

Acknowledgments—We thank the following scientists for providing cDNA clones: Dr. David Julius (University of California San Francisco) for the rat TRPV1 clone, Dr. Makoto Tominaga (National Institute for Physiological Sciences) for the S502A/S800A rTRPV1 mutant, Dr. Thomas Hughes (Montana State University) for the Green-up (DAG)/Red-GECO (Ca^{2+}) sensor, and Dr. Tamas Balla (National Institutes of Health) for the PKDc1ab-GFP DAG sensor and PLCPHδ-RFP $PI(4,5)P_2$ sensor.

Author contributions—L. L. and T. R. conceptualization; L. L. and Y. Y. data curation; L. L. and Y. Y. formal analysis; L. L. and Y. Y. investigation; L. L. visualization; L. L. and T. R. writing-original draft; L. L., Y. Y., and T. R. writing-review and editing; T. R. supervision; T. R. funding acquisition; T. R. project administration.

Funding and additional information—This work was supported by NINDS, National Institutes of Health Grants NS055159 and NIGMS, National Institutes of Health Grants GM131048 and GM093290 (to T. R.). The content is solely the responsibility of the authors and does not necessarily represent the official views of the National Institutes of Health.

Conflict of interest—The authors declare that they have no conflicts of interest with the contents of this article.

Abbreviations—The abbreviations used are: DRG, dorsal root ganglia; PLC, phospholipase C; $PI(4,5)P_2$, phosphatidylinositol 4,5-bisphosphate; DAG, diacylglycerol; DAGK, diacylglycerol kinase; DAGL, diacylglycerol lipase; BIM-IV, bisindolylmaleimide IV; PI(4)P, phosphatidylinositol 4-phosphate; PKC, protein kinase C; EC, extracellular.

References

1. Caterina, M. J., Schumacher, M. A., Tominaga, M., Rosen, T. A., Levine, J. D., and Julius, D. (1997) The capsaicin receptor: a heat-activated ion channel in the pain pathway. *Nature* **389,** 816–824 CrossRef Medline

2. Cesare, P., and McNaughton, P. (1996) A novel heat-activated current in nociceptive neurons and its sensitization by bradykinin. *Proc. Natl. Acad. Sci. U.S.A.* **93,** 15435–15439 CrossRef Medline
3. Tominaga, M., Wada, M., and Masu, M. (2001) Potentiation of capsaicin receptor activity by metabotropic ATP receptors as a possible mechanism for ATP-evoked pain and hyperalgesia. *Proc. Natl. Acad. Sci. U.S.A.* **98,** 6951–6956 CrossRef Medline
4. Numazaki, M., Tominaga, T., Toyooka, H., and Tominaga, M. (2002) Direct phosphorylation of capsaicin receptor VR1 by protein kinase Cε and identification of two target serine residues. *J. Biol. Chem.* **277,** 13375–13378 CrossRef Medline
5. Joseph, J., Qu, L., Wang, S., Kim, M., Bennett, D., Ro, J., Caterina, M. J., and Chung, M. K. (2019) Phosphorylation of TRPV1 S801 contributes to modality-specific hyperalgesia in mice. *J. Neurosci.* **39,** 9954–9966 CrossRef Medline
6. Koplas, P. A., Rosenberg, R. L., and Oxford, G. S. (1997) The role of calcium in the desensitization of capsaicin responses in rat dorsal root ganglion neurons. *J. Neurosci.* **17,** 3525–3537 CrossRef Medline
7. Yao, J., and Qin, F. (2009) Interaction with phosphoinositides confers adaptation onto the TRPV1 pain receptor. *PLoS Biol.* **7,** e46 CrossRef Medline
8. Lukacs, V., Yudin, Y., Hammond, G. R., Sharma, E., Fukami, K., and Rohacs, T. (2013) Distinctive changes in plasma membrane phosphoinositides underlie differential regulation of TRPV1 in nociceptive neurons. *J. Neurosci.* **33,** 11451–11463 CrossRef Medline
9. Borbiro, I., Badheka, D., and Rohacs, T. (2015) Activation of TRPV1 channels inhibit mechanosensitive Piezo channel activity by depleting membrane phosphoinositides. *Sci. Signal.* **8,** ra15 CrossRef Medline
10. Lukacs, V., Thyagarajan, B., Varnai, P., Balla, A., Balla, T., and Rohacs, T. (2007) Dual regulation of TRPV1 by phosphoinositides. *J. Neurosci.* **27,** 7070–7080 CrossRef Medline
11. Rohacs, T. (2015) Phosphoinositide regulation of TRPV1 revisited. *Pflugers Arch.* **467,** 1851–1869 CrossRef Medline
12. Cesare, P., Dekker, L. V., Sardini, A., Parker, P. J., and McNaughton, P. A. (1999) Specific involvement of PKC-ε in sensitization of the neuronal response to painful heat. *Neuron* **23,** 617–624 CrossRef Medline
13. Zhang, X., Li, L., and McNaughton, P. A. (2008) Proinflammatory mediators modulate the heat-activated ion channel TRPV1 via the scaffolding protein AKAP79/150. *Neuron* **59,** 450–461 CrossRef Medline
14. Sato, M., Liu, K., Sasaki, S., Kunii, N., Sakai, H., Mizuno, H., Saga, H., and Sakane, F. (2013) Evaluations of the selectivities of the diacylglycerol kinase inhibitors R59022 and R59949 among diacylglycerol kinase isozymes using a new non-radioactive assay method. *Pharmacology* **92,** 99–107 CrossRef Medline
15. Tewson, P. H., Quinn, A. M., and Hughes, T. E. (2013) A multiplexed fluorescent assay for independent second-messenger systems: decoding GPCR activation in living cells. *J. Biomol. Screen* **18,** 797–806 CrossRef Medline
16. Thams, P., and Capito, K. (1997) Inhibition of glucose-induced insulin secretion by the diacylglycerol lipase inhibitor RHC 80267 and the phospholipase A2 inhibitor ACA through stimulation of K^+ permeability without diminution by exogenous arachidonic acid. *Biochem. Pharmacol.* **53,** 1077–1086 CrossRef Medline
17. Kim, Y. J., Guzman-Hernandez, M. L., and Balla, T. (2011) A highly dynamic ER-derived phosphatidylinositol-synthesizing organelle supplies phosphoinositides to cellular membranes. *Dev. Cell* **21,** 813–824 CrossRef Medline
18. Boroda, S., Niccum, M., Raje, V., Purow, B. W., and Harris, T. E. (2017) Dual activities of ritanserin and R59022 as DGKα inhibitors and serotonin receptor antagonists. *Biochem. Pharmacol.* **123,** 29–39 CrossRef Medline
19. Ogasawara, D., Deng, H., Viader, A., Baggelaar, M. P., Breman, A., den Dulk, H., van den Nieuwendijk, A. M., Soethoudt, M., van der Wel, T., Zhou, J., Overkleeft, H. S., Sanchez-Alavez, M., Mori, S., Nguyen, W., Conti, B., *et al.* (2016) Rapid and profound rewiring of brain lipid signaling networks by acute diacylglycerol lipase inhibition. *Proc. Natl. Acad. Sci. U.S.A.* **113,** 26–33 CrossRef Medline
20. Liu, X., Wang, Y., Zhang, H., Shen, L., and Xu, Y. (2017) Different protein kinase C isoenzymes mediate inhibition of cardiac rapidly activating delayed rectifier K^+ current by different G-protein coupled receptors. *Br. J. Pharmacol.* **174,** 4464–4477 CrossRef Medline
21. Mandadi, S., Numazaki, M., Tominaga, M., Bhat, M. B., Armati, P. J., and Roufogalis, B. D. (2004) Activation of protein kinase C reverses capsaicin-induced calcium-dependent desensitization of TRPV1 ion channels. *Cell Calcium* **35,** 471–478 CrossRef Medline
22. Mandadi, S., Tominaga, T., Numazaki, M., Murayama, N., Saito, N., Armati, P. J., Roufogalis, B. D., and Tominaga, M. (2006) Increased sensitivity of desensitized TRPV1 by PMA occurs through PKCε-mediated phosphorylation at S800. *Pain* **123,** 106–116 CrossRef Medline
23. Tewson, P., Westenberg, M., Zhao, Y., Campbell, R. E., Quinn, A. M., and Hughes, T. E. (2012) Simultaneous detection of Ca^{2+} and diacylglycerol signaling in living cells. *PLoS ONE* **7,** e42791 CrossRef Medline
24. Tu-Sekine, B., Goldschmidt, H., and Raben, D. M. (2015) Diacylglycerol, phosphatidic acid, and their metabolic enzymes in synaptic vesicle recycling. *Adv. Biol. Regul.* **57,** 147–152 CrossRef Medline
25. Lee, M. W., and Severson, D. L. (1994) Signal transduction in vascular smooth muscle: diacylglycerol second messengers and PKC action. *Am. J. Physiol.* **267,** C659–C678 CrossRef Medline
26. Shirai, Y., and Saito, N. (2014) Diacylglycerol kinase as a possible therapeutic target for neuronal diseases. *J. Biomed. Sci.* **21,** 28 CrossRef Medline
27. Jiang, Y., Sakane, F., Kanoh, H., and Walsh, J. P. (2000) Selectivity of the diacylglycerol kinase inhibitor 3-[2-(4-[bis-(4-fluorophenyl)methylene]-1-piperidinyl)ethyl]-2,3-dihydro-2-thioxo-4(1H)quinazolinone (R59949) among diacylglycerol kinase subtypes. *Biochem. Pharmacol.* **59,** 763–772 CrossRef Medline
28. Tu-Sekine, B., Goldschmidt, H., Petro, E., and Raben, D. M. (2013) Diacylglycerol kinase theta: regulation and stability. *Adv. Biol. Regul.* **53,** 118–126 CrossRef Medline
29. Baldanzi, G., Alchera, E., Imarisio, C., Gaggianesi, M., Dal Ponte, C., Nitti, M., Domenicotti, C., van Blitterswijk, W. J., Albano, E., Graziani, A., and Carini, R. (2010) Negative regulation of diacylglycerol kinase θ mediates adenosine-dependent hepatocyte preconditioning. *Cell Death Differ.* **17,** 1059–1068 CrossRef Medline
30. Epand, R. M., So, V., Jennings, W., Khadka, B., Gupta, R. S., and Lemaire, M. (2016) Diacylglycerol kinase-ε: properties and biological roles. *Front. Cell Dev. Biol.* **4,** 112 CrossRef Medline
31. Lung, M., Shulga, Y. V., Ivanova, P. T., Myers, D. S., Milne, S. B., Brown, H. A., Topham, M. K., and Epand, R. M. (2009) Diacylglycerol kinase ε is selective for both acyl chains of phosphatidic acid or diacylglycerol. *J. Biol. Chem.* **284,** 31062–31073 CrossRef Medline
32. Walsh, J. P., Suen, R., and Glomset, J. A. (1995) Arachidonoyl-diacylglycerol kinase: specific *in vitro* inhibition by polyphosphoinositides suggests a mechanism for regulation of phosphatidylinositol biosynthesis. *J. Biol. Chem.* **270,** 28647–28653 CrossRef Medline
33. Thirugnanam, S., Topham, M. K., and Epand, R. M. (2001) Physiological implications of the contrasting modulation of the activities of the ε- and ζ-isoforms of diacylglycerol kinase. *Biochemistry* **40,** 10607–10613 CrossRef Medline
34. Suh, B. C., and Hille, B. (2006) Does diacylglycerol regulate KCNQ channels? *Pflugers Arch.* **453,** 293–301 CrossRef Medline
35. Raghu, P., Usher, K., Jonas, S., Chyb, S., Polyanovsky, A., and Hardie, R. C. (2000) Constitutive activity of the light-sensitive channels TRP and TRPL in the *Drosophila* diacylglycerol kinase mutant, rdgA. *Neuron* **26,** 169–179 CrossRef Medline
36. Liu, L., Yudin, Y., Nagwekar, J., Kang, C., Shirokova, N., and Rohacs, T. (2019) $G\alpha_q$ sensitizes TRPM8 to inhibition by $PI(4,5)P_2$ depletion upon receptor activation. *J. Neurosci.* **39,** 6067–6080 CrossRef Medline